



Application Note AN-BAT-015

# Differential capacity analysis (DCA) for battery research with INTELLO

Introducing  $dQ/dE$  plots, applications, and more

Differential capacity analysis (DCA) is a powerful diagnostic technique widely used in battery research and development to gain detailed insights into the electrochemical behavior of batteries. DCA allows researchers to identify key electrochemical processes, phase transitions, and degradation mechanisms occurring within the battery during charge and discharge cycles. This technique is particularly valuable for characterizing complex systems such as lithium-ion batteries, where multiple electrochemical

reactions may overlap.

This Application Note explores the principles and practical applications of differential capacity analysis, highlighting its role in improving battery performance. This application also reveals how INTELLO, with its dedicated suite of battery-oriented commands and its ability to untether during long measurements, is an excellent choice for battery researchers looking to maximize their time and efficiency when conducting DCA.

## INTRODUCTION

Within the INTELLO battery cycling environment, it is possible to sample the differential capacity (defined as  $dQ/dE = |Q_{n+1} - Q_n| / (E_{n+1} - E_n)$ , where  $n$  is the index of the data point,  $Q$  is the value of the charge/discharge capacity, and  $E$  is the measured working electrode potential) and plot by default this value versus the

measured voltage of the cell. Note that a general introduction to the cycling environment in INTELLO is provided in [AN-BAT-014](#) while this Application Note specifically focuses on the  $dQ/dE$  plot and what can be derived from it.

## SAMPLE DETAILS AND PREPARATION

Four commercially available batteries containing different cathode materials were studied with

charge/discharge cycling and DCA. The details of samples 1–4 can be found in [Table 1](#).

**Table 1.** Details of the four battery sample types used in this study.

Sample	Form	Identifying Code	Capacity / mAh
1	Coin-cell	LIR2450	120
2	Cylinder	INR21700-33J	3200
3	Cylinder	HTPFPR-18650	1100
4	Cylinder	BK-3MCDE	2000

## RESULTS AND DISCUSSION

In general, DCA is performed at low C-rates (C/10 or lower). This is especially required when DCA is done to understand fundamental electrochemical processes inside the battery. Each peak in a  $dQ/dE$  plot corresponds to an electrochemical or an electrochemically induced process, e.g., phase changes in the cathode material or Li intercalation into graphite. It is important that the C-rate is low so that the most accurate voltage can be determined. It

also gives the battery sufficient time to reach equilibrium at each voltage step and therefore allows different electrochemical processes to be fully resolved from one another, leading to more distinct peaks with less overlap and broadening. Higher C-rates can suppress or obscure processes which occur on a slower timescale, so it is not uncommon to detect entirely new peaks at lower C-rates.

## LIR2450 COIN CELL BATTERY

The cell was cycled at 1C and 0.1C. The charge limit was 4.2 V, the current-cutoff 6 mA, and the discharge limit 2.8 V. To illustrate the differences which can occur between C-rates, **Figure 1** shows overlaid data of the differential capacity plots from cycling at 0.1C (in blue) and at 1C (in green).

At 1C, two peaks appear at 3.82 V (A1) and at 3.95 V (A2) during the charging step, and one peak at 3.62 V (B1'') during the discharge. At 0.1C, even more detail is shown. The charge portion of the plot displays four peaks at 3.70 V (A1), 3.77 V (A1\*), 3.81 V (A2), and 3.93 V (A2\*), while the discharge segment has two peaks: one at 3.64 V (B1) and one at 3.75 V (B2). This data is summarized in **Table 2** and is consistent with a battery containing an NMC-532 cathode [1].

One possible explanation of the differences in the plots of the two C-rates could be that peaks A1 and A2 at 1C are shifting to a lower overpotential when the battery is charged at 0.1C, reflecting the increased efficiency of the charging process, while the new peaks of A1\* and A2\* could be related to reactions with slow kinetics that are obscured at higher C-rates. The peak seen during discharge at 1C is resolved into two sharper peaks at 0.1C. Most likely, both peaks are linked to the two major phase transitions seen in the charging portion at both C-rates.

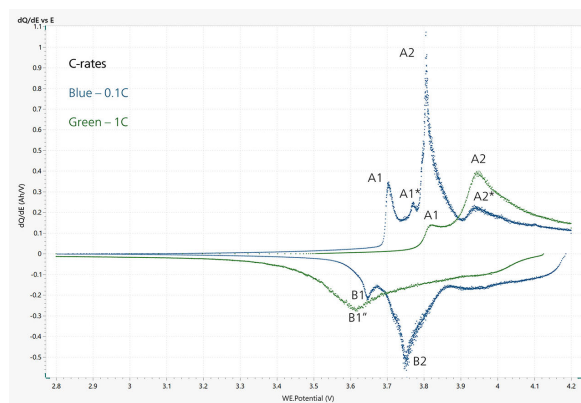


**Figure 1.** dQ/dE plots of a Li-coin cell battery at 0.1C (blue) and 1C (green).

**Table 2.** Positions of the peaks observed in Figure 1.

Peak	Peak Position (V)	
	0.1C	1C
A1	3.70	3.82
A1*	3.77	-
A2	3.81	3.95
A2*	3.93	-
B1''	-	3.62
B1	3.64	-
B2	3.75	-

Plateaus in the E vs Q+/Q- plot also indicate phase changes and electrochemical processes. However, plateaus are not always so easy to detect in this plot. In **Figure 2**, the corresponding E vs Q+/Q- plot is shown for the 0.1C cycle. Plateaus are shown as peaks in the dQ/dE plot, making them much easier to detect, and highlighting one of the benefits of representing the data in this way.

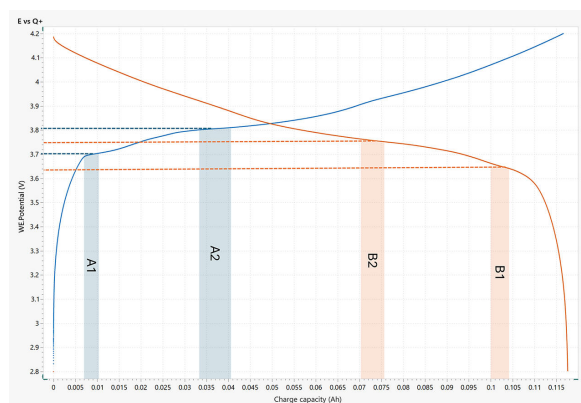


**Figure 2.** E vs Q+/Q- plot of a Li-coin cell battery where the corresponding plateaus that give rise to the peaks in the dQ/dE plot are highlighted. Plateaus represent phase changes in the active material.

Another possible use of the dQ/dE plot is to track changes in the chemistry of the battery as it is cycled over a longer period of time. In **Figure 3**, the same type of battery was cycled 100 times at 1C and the dQ/dE signal was collected and plotted in INTELLO. The changes in peak height and position give clues to the possible degradation mechanisms at work in the battery. In this example, the peak height is reducing and the peak itself is also shifting, which usually indicates a loss of Li inventory. Therefore, possible aging mechanisms could include things like Li plating or electrolyte decomposition. Other examples that can be detected using DCA include conductivity loss, indicated by the peaks shifting to higher voltages (i.e., more overpotential required for same work), and loss of active material, revealed by reduction in peak height but without a shift in the peak position.

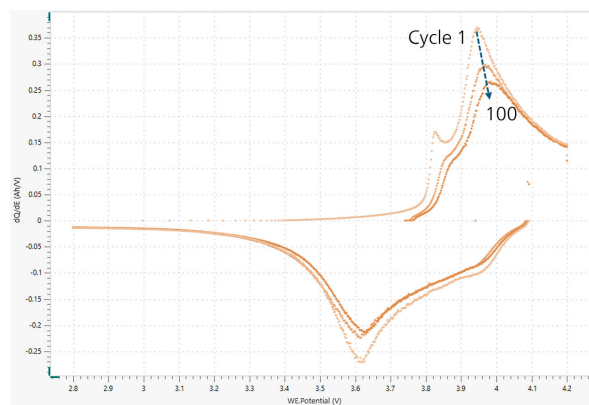


**Figure 3.** dQ/dE plot of a Li-ion coin cell battery after 1 cycle, 50 cycles, and 100 cycles. The more cycles, the darker the line color in this plot.

## INR21700-33J LI ION CYLINDER BATTERY

A standard charge/discharge cycle for this battery consists of a CCCV charging step followed by a CC discharge. Initially, the battery is charged at 0.5C to 4.2 V. The voltage is held until the current has dropped below 64 mA (0.02C). The cell is then discharged at 0.2C to 3 V. In theory, the battery should be charged and discharged at the same C-rate to ensure the charge and discharge curves are more directly comparable, but in this case the plot was collected during a standard charge in order to observe the electrochemical processes *in situ*, under normal cycling conditions.

In **Figure 4**, three peaks appear in the charge portion at 3.58 V (C1), 3.60 V (C1\*), and 3.72 V (C2). During the discharge of the battery, three peaks are also detected at 3.44 V (D1), 3.58 V (D2), and a broad peak noted as D3.

The overall structure of the plot is very similar to **Figure 1** measured with the coin cell meaning that, despite the larger form factor, the chemistry in this battery is rather similar to the coin cell battery described earlier. From the dQ/dE plot we can tell that it likely also contains an NMC-type cathode. Since the ratio of the peaks is also similar, it is possible that it is the same material.

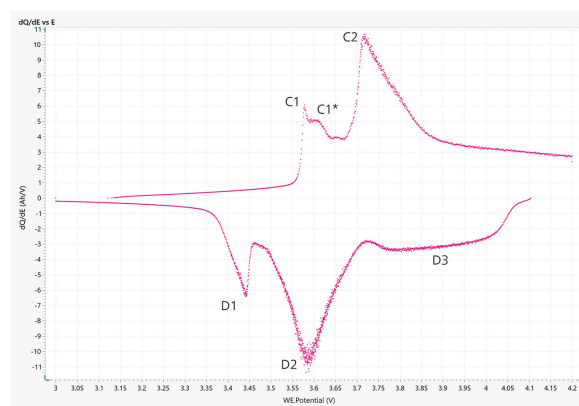


**Figure 4.** dQ/dE plot of a Li-ion cylinder battery.

## HTPFPR-18650 LI ION CYLINDER BATTERY

For this analysis, the battery was cycled with a CC charge/discharge procedure at 1C, and the voltage limit on the charge sweep was slowly expanded to capture all the dQ contributions separately. Initially, the battery was first charged to 3.35 V and then discharged to 2.8 V. The battery was then charged/discharged three more times to 3.38 V, 3.42 V, and 3.65 V. This is plotted in **Figure 5**.

The chemistry of this battery is known to be based on lithium iron phosphate (LFP) which can also be confirmed from the lower upper voltage limit compared to the preceding two batteries. Also, this can be confirmed from the dQ/dE plot which has a characteristic shape.

The charging section consists of four peaks at 3.32 V (E1), 3.38 V (E2), 3.40 V (E3), and 3.44 V (E4). The discharging section also contains four peaks at 3.11 V (F1), 3.15 V (F2), 3.19 V (F3), and 3.24 V (F4). The peaks in both sections can be linked to one another even better by increasing the voltage limit each time. The shape of this curve and the observed peaks are consistent with an LFP/graphite type battery. Peaks E3 and E4 (and the corresponding F3 and F4) most likely are related to Li-ion (de)intercalation, while the other peaks are related to phase changes in the LFP/graphite [2].

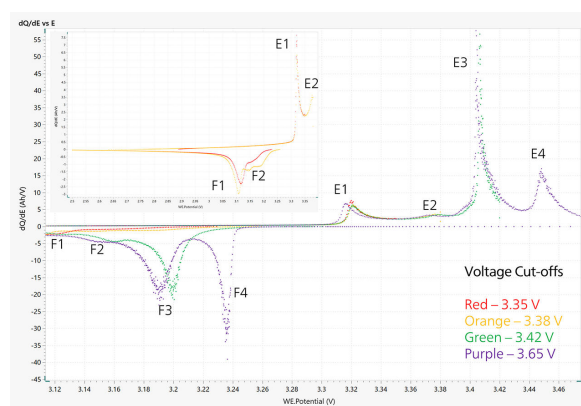


**Figure 5.** dQ/dE plot of an HTPFPR-18650 cylinder battery cycled at different voltage limits. Insert: magnified section of the curve between 2.28 and 3.38 V.

## BK-3MCDE/4BE NI-MH CYLINDER BATTERY

The final battery tested in this study was a Ni-MH cylinder battery. This battery was cycled with CC charge and discharge at 0.1C between 1 V and 1.5 V. The dQ/dE plot is shown in **Figure 6**.

The chemistry of this battery is dominated in this region by the conversion of  $\text{Ni}(\text{OH})_2$  to  $\text{NiOOH}$  and its reverse during the discharge. As such, only one peak is seen at 1.4 V on the charge curve, and one peak is observed on the discharge curve at 1.28 V. Another Application Note ([AN-RS-042](#)) also shows how it is possible to follow this reaction with in-situ Raman spectroelectrochemistry.

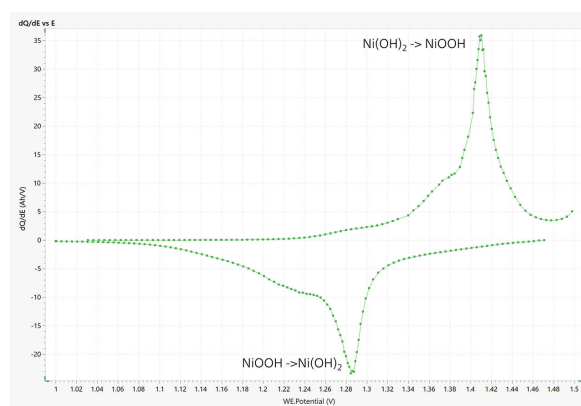


**Figure 6.** dQ/dE plot of the Ni-MH battery cycled at 0.1C.

## REFERENCES

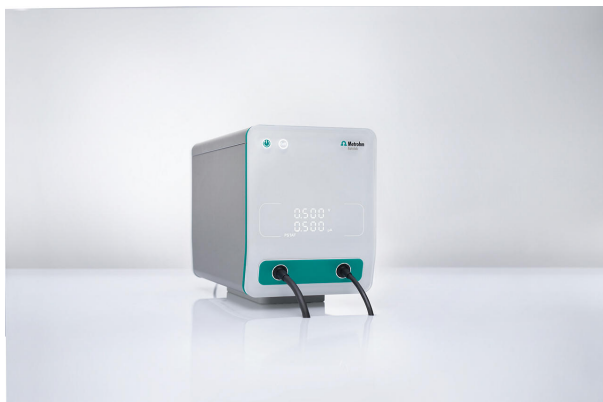
1. Long, B. R.; Rinaldo, S. G.; Gallagher, K. G.; et al. Enabling High-Energy, High-Voltage Lithium-Ion Cells: Standardization of Coin-Cell Assembly, Electrochemical Testing, and Evaluation of Full Cells. *J. Electrochem. Soc.* **2016**, *163* (14), A2999. DOI:10.1149/2.0691614jes
2. Torai, S.; Nakagomi, M.; Yoshitake, S.; et al. State-of-Health Estimation of LiFePO<sub>4</sub>/Graphite Batteries Based on a Model Using Differential Capacity. *J. Power Sources* **2016**, *306*, 62–69. DOI:10.1016/j.jpowsour.2015.11.070

## CONTACT

Metrohm France  
13, avenue du Québec - CS  
90038  
91978 VILLEBON  
COURTABOEUF CEDEX

info@metrohm.fr

## CONFIGURATION



### VIONIC

VIONIC est notre potentiostat/galvanostat de dernière génération piloté par le nouveau logiciel d'Autolab, INTELLO.

VIONIC offre les **spécifications combinées les plus polyvalentes pour un appareil unique** actuellement sur le marché.

- Tension disponible :  $\pm 50$  V
- Intensité standard :  $\pm 6$  A
- Fréquence de SIE : jusqu'à 10 MHz
- Intervalle d'échantillonnage : jusqu'à 1  $\mu$ s

Le prix de VIONIC inclut également des fonctions qui impliquent généralement des coûts supplémentaires avec la plupart des autres appareils, telles que :

- Spectroscopie d'impédance électrochimique (SIE)
- Mode flottant sélectionnable
- Seconde électrode de détection (S2)
- Scan analogique